Structural studies of ambient temperature plastic crystal ion conductors

2001 J. Phys.: Condens. Matter 13 8257

(http://iopscience.iop.org/0953-8984/13/36/303)

INSTITUTE OF PHYSICS PUBLISHING JOURNAL OF PHYSICS: CONDENSED MATTER

J. Phys.: Condens. Matter **13** (2001) 8257–8267 PII: S0953-8984(01)23777-1

Structural studies of ambient temperature plastic crystal ion conductors

D R MacFarlane[1], P Meakin[1], N Amini[1] and M Forsyth[2]

[1] School of Chemistry, Monash University, Victoria 3800, Australia
[2] School of Physics and Materials Engineering, Monash University, Victoria 3800, Australia

Received 9 April 2001
Published 23 August 2001
Online at stacks.iop.org/JPhysCM/13/8257

Abstract

A number of novel organic ionic compounds based on the pyrrolidinium cation are described which have been found to be ion conductors in their solid states around room temperature. The properties of the compounds are consistent with their exhibiting plastic crystal phases. In order to understand some of the molecular origins of the plastic crystal behaviour and the ion conductivity that it promotes, a number of related compounds based on the imidazolium and ammonium cations are also described which have structural elements in common with the pyrrolidinium cation, but which do not show the plastic behaviour. It is found therefore that the nature of the cation is quite critical to the development of this behaviour. The alkyl methyl pyrrolidinium cation is found to produce plastic crystal phases when the alkyl chains are short, thereby preserving the ability of the cation to rotate with minimal steric hindrance. The ammonium and imidazolium cations of comparable size and structure are less able to produce these plastic phases, in many cases because the low temperature phase proceeds to melt rather than forming a stable rotator phase.

1. Introduction

Solid state ion conductors have been of perennial interest because of their application in electrochemical devices such as batteries and fuel cells. In the field of rechargeable batteries there is a need for ambient temperature ion conductive materials that are preferably solid and of low vapour pressure such that loss and leakage of electrolyte is limited and flammability issues are minimized. Much attention has been devoted in recent years to the preparation and properties of solid polymer electrolytes formed by dissolving salts into a polar polymer medium such as polyethyleneoxide [1, 2]. However the conductivity of these materials typically lies in the region 10^{-6}–10^{-4} S cm^{-1} at room temperature, the dynamics of ion motion being limited by the association of the ions with the polymer backbone. The latter is typically mobile (that is the polymer is above T_g) at room temperature, but not sufficiently so to facilitate high conductivity. The ion conduction in such materials is often described as strongly coupled (even super-coupled) to the structural modes of motion [3]. At the other extreme, in terms

of coupling, are materials which are conductive at room temperature by virtue of a fast ion motion of one ion, for example a small cation such as lithium, in a glassy or crystalline matrix which is translationally static. For example lithium titanium phosphate ceramics exhibit Li^+ ion conductivity as high as 10^{-3} S cm^{-1} at room temperature [4].

An intermediate state of coupling between conductive and structural modes of motion has been observed recently by a number of groups including ours, in a group of organic plastic crystalline materials [5–12]. Plastic phases have been known since the time of Timmermans [13]. Such phases can be thought of as an intermediate state of matter, possessing limited translational motion of the constituent molecules, though nonetheless maintaining a definite three dimensional crystalline lattice. The presence of diffusional modes of motion allows the materials to exhibit plastic flow under stress, hence the term plastic crystal [13]. The plastic phase or phases of the substance are often reached via solid–solid phase transitions below the final melting point of the crystal; in these cases the solid–solid transition represents the onset of rotational motions of the molecules within the crystalline lattice. Such phases are often referred to as rotator phases—rotator phases generally possess plastic properties; however the latter behaviour can also originate in other ways. Timmermans proposed a general rule that plastic phases normally have a low final entropy of fusion ($\Delta S_f < 20$ J K^{-1} mol^{-1}) as a result of the fact that the rotational component of the entropy of fusion of the fully ordered phase is already present in the plastic phase.

A number of ionic compounds are known to exhibit plastic properties. In such cases the diffusional degrees of freedom active in the higher temperature phases can produce ion conductivity. Examples include Li_2SO_4 [14] in which the rotatory motions of the SO_4^{2-} anion in the plastic phase facilitate the motion of the Li ions via a paddle wheel type mechanism, thus producing quite substantial ion conductivity at elevated temperatures. Ambient temperature ion conduction has been observed by us [5] and others [6–11] in organic compounds such as [5] the methylethylpyrrolidinium cation (I) salt of the bis(trifluoromethanesulphonyl) amide (TFSA) anion (II). In these cases the nature of the conduction process, or the identity of the conducting ion or ions has yet to be unambiguously determined. What is clear is that the rotatory motions of one or both of the ions facilitates translation of a subset of the ions in the crystal lattice.

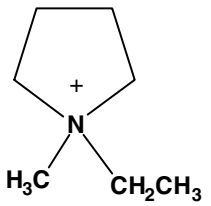

(I)

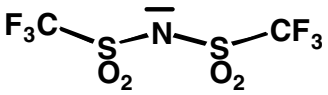

(II)

An interesting doped ion effect has also been observed by us [12, 15] in which small cations such as Li, when present at relatively low concentrations, can produce quite substantial increases in conductivity—up to two orders of magnitude. Such doped plastic crystal conductors are of both practical interest, since the conductivity is high enough at room temperature ($\sigma = 10^{-4}$ S cm^{-1}) to be of interest in practical devices, and also fundamentally since they represent a new class of fast ion conductive materials.

The origins of the rotatory motions which are the progenitor of all of these interesting properties are nonetheless obscure in these compounds. It is not possible to predict *a priori* which compound will exhibit such rotator phases, or even necessarily which of the ions in an

ionic compound will be involved. To investigate this further in this work we have prepared a number of structurally related compounds for the purpose of examining the structural origins of the plastic crystal and conductive behaviour exhibited by some of the compounds. Salts from the ammonium (III), pyrrolidinium (IV) and imidazolium (V) cation families are described and their properties compared. Similarly a number of salts of the same cation but of different anions, including the TFSA and iodide anions are described and compared.

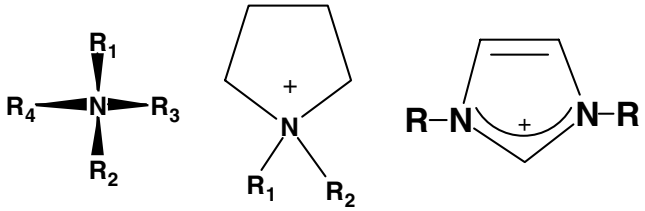

(III) (IV) (V)

R_1, R_2, R_3 and R_4 are alkyl chains such as methyl, ethyl, propyl etc.

2. Experiment

The compounds were prepared and characterized by methods reported previously [16–18]. The salts prepared are summarized in table 1 along with the acronym used to identify the compounds. To distinguish between the cations in these compounds we use an acronym in which P = pyrrolidinium, Im = imidazolium and N = ammonium and the subscripts indicate the number of CH_2 units in each of the attached alkyl chains. Salts of the triflate anion were also prepared by the same methods, substituting the triflate anion for the TFSA anion in the synthesis. All compounds were dried under vacuum at 45 °C for at least 24 hours before measurements were made. Thermal analysis was carried out on a Perkin Elmer differential scanning calorimeter model DSC-7. The DSC was calibrated at ambient temperatures and above (50–200 °C) with indium (156.54 °C) and *p*-nitrotoluene (51.64 °C) and below ambient using the solid–solid transitions in cyclohexane.

Conductivity was obtained using a locally designed conductivity cell which consisted of an aluminium block into which six symmetrically arranged sample wells were machined. Stainless steel inserts into these sample wells formed one of the electrodes for the measurements. The other electrode consisted of a stainless steel cylinder located in the centre of the well by Teflon spacers such that the sample consisted of a 0.2 mm thick annulus approximately 5 cm in length. The effective cell constant, b, of this arrangement was estimated from geometric considerations to be approximately 0.0025 cm^{-1}. The actual cell constant of the cell was obtained by measurement of the empty capacitance, C_0, of the cell as a function of frequency and calculation of b via

$$bn = \varepsilon_0 / C_0$$

where ε_0 = the permittivity of free space.

The conductivity cell also contained a cartridge heater and a control/measurement thermocouple well such that the temperature of the cell could be controlled by a Eurotherm temperature controller to within 0.1 °C of set temperature.

In a typical conductivity run the sample was melted and poured into the conductivity cell which was then sealed and quenched into liquid nitrogen. The cell was then placed in an

Table 1. Thermal properties of the pyrrolidinium, ammonium and imidazolium compounds.

Compound	Acronym	T_g (°C) ±2 °C	T_{s-s} (°C) ±2 °C	T_m (°C) ±2 °C	ΔS_f (J K^{-1} mol^{-1}) ±5%
Dimethyl pyrrolidinium TFSA	P_{11}TFSA	—	20	132	40
Ethylmethyl pyrrolidinium TFSA	P_{12}TFSA	−90 ? (plastic crystal)	−90 ? 18 45	88	38
Propylmethyl pyrrolidinium TFSA	P_{13}TFSA	−90	−18	12	43
Butylmethyl pyrrolidinium TFSA	P_{14}TFSA	−87	−24	−18	41
Pentylmethyl pyrrolidinium TFSA	P_{15}TFSA	−83	4	8	∼80
Hexylmethyl pyrrolidinium TFSA	P_{16}TFSA	−87		3	[a]
Dimethylethylpropyl ammonium TFSA	N_{1123}TFSA	−92	—	−10	82
Trimethylbutyl ammonium TFSA	N_{1114}TFSA	−83	9	16	∼22[b]
Dimethylpropylbutyl ammonium TFSA	N_{1134}TFSA	−85	shoulder	20	53
Octyltriethyl ammonium TFSA	N_{8222}TFSA	−80	—	14 (weak)	[a]
Ethylmethyl imidazolium TFSA	I_{12}TFSA	−95	—	−16	84
Butylmethyl imidazolium TFSA	I_{14}TFSA	−87	—	−1	[a]
Butylmethyl imidazolium iodide	I_{14} iodide	−85	—	—	—

[a] Accurate entropy data not obtainable due to evidence of incomplete crystallization.
[b] Estimate only, due to overlap between s–s and melting transitions.

insulated container which was itself placed in a liquid nitrogen containing dewar. The cell was heated at a constant rate of 0.3 °C min^{-1} during the measurement run. This is expected to produce a slight lag (∼1 °C) such that the actual sample temperature is slightly lower than the thermocouple temperature; however over the wide temperature ranges covered in this study this is a minor effect. Impedance measurements were made at regular temperature intervals during the heating run, typically from −120 °C to 100 °C. Replicate runs were carried out to verify reproducibility of the effects. Carrying out conductivity runs during cooling produced a variety of hysteresis effects attributable to undercooling of the various phases; for this reason the slow warming runs carried out here are more reproducible.

Impedance measurements were carried out using an HP impedance analyser over the frequency range from 20 Hz to 1 MHz. The frequency analyser and temperature controller were actively controlled by a Macintosh computer. The conductivity was obtained from the resistance of the real axis intercept of the data plotted in impedance plane format. The impedance plane plot showed only a single semicircle followed by a low frequency electrode spike.

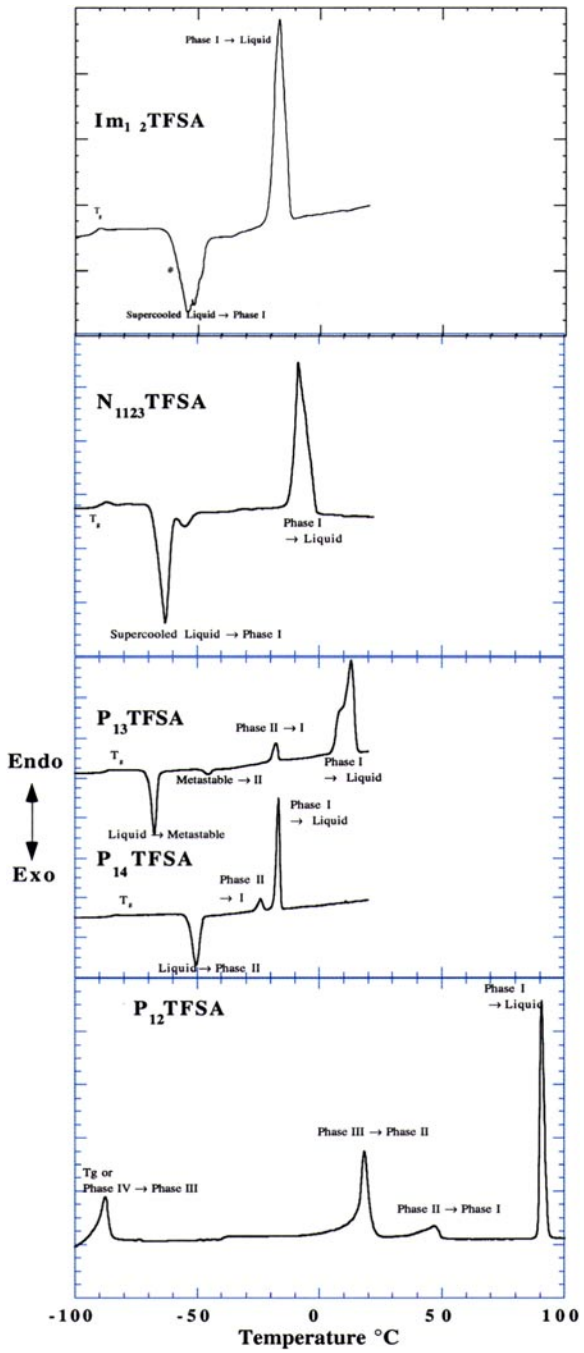

Figure 1. DSC Thermal analysis trace of a number of different TFSA salts from the pyrrolidinium, ammonium and imidazolium families.

3. Results

Figure 1 presents a number of DSC thermograms illustrating the range of behaviours observed for these compounds. The P_{12}TFSA case is archetypal of a compound showing several solid–

solid transitions below the melting point. On the other hand, a number of compounds exhibit distinct glass transitions, after quenching in the DSC, followed by classical devitrification event (crystallization during warming) and only a single endotherm corresponding to the melting transition. Thermal data extracted from the thermograms are summarized in table 1. The entropy of fusion values, where they can be obtained, fall into two clear groups; those around or below 40 J K^{-1} mol^{-1} and those around 80 J K^{-1} mol^{-1}. None of the compounds satisfy Timmerman's criterion, $\Delta S_f < 20$ J K^{-1} mol^{-1} for plastic crystal behaviour. We have argued previously that this criterion, as originally developed by Timmermans, is only appropriate for simple molecular crystalline materials. In the present case of compounds which contain two distinct molecular ions, the situation may be more complex. Where only one of the ions (the cation or the anion) is involved in the rotatory motions in the solid state and the other ion possesses a number of rotatory degrees of freedom that become active on melting, we can expect a higher residual entropy of fusion. This hypothesis has been supported recently by the observation of entropies of fusion in the vicinity of 20 J K^{-1} mol^{-1} for a number of methyl alkyl pyrrolidinium hexafluorophosphate salts [19], the simple symmetrical anion in this case allowing the plastic crystal phases to involve motions of both ions. Thus in the present case entropies of melting in the vicinity of 40 J K^{-1} mol^{-1}, along with the existence of sub-melting solid–solid phase transitions are taken as indicative of the presence of rotator phases prior to melting. On the other hand entropies of melting in the vicinity of 80 J K^{-1} mol^{-1} plus a lack of such transitions are taken to indicate a fully static crystalline phase up to the melting point.

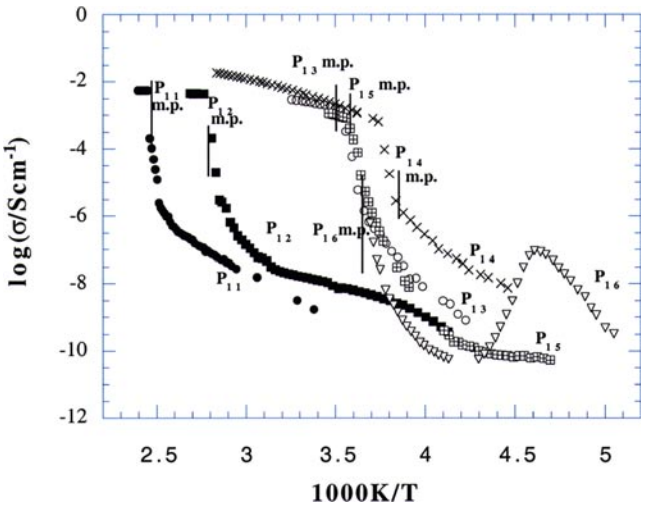

Figure 2. Arrhenius plot of conductivity for the alkyl methyl pyrrolidinium TFSA family of compounds P_{11}TFSA to P_{16}TFSA. The melting point of each compound is indicated also. The dashed curve joins high and low temperature regions of the liquid state of P_{15}TFSA.

Figure 2 presents typical conductivity behaviour of a family of related compounds, in this case the alkyl methyl pyrrolidinium TFSA family. The Arrhenius format is used to present the data; on this plot a simple, single activation energy, conduction process would appear as a straight line. The structural variable in this family is the length of the alkyl group, R, which in this case varies between one and six CH_2 units. In the case of figure 2 the conductivity behaviour of P_{11}TFSA–P_{14}TFSA has been described previously [5]; here we supplement this with two further members of the family which also show conductive behaviour.

The salts in this family show an interesting range of behaviours, best exemplified by

P_{12}TFSA. This salt melts into a fluid liquid of conductivity in excess of 10^{-2} S cm^{-1} at 90 °C, but above −50 °C it is measurably conductive in the solid state and exhibits conductivity around 10^{-6} S cm^{-1} throughout the ambient temperature region up to shortly below the melting point. P_{11}TFSA and P_{13}TFSA show similarly conductive solid states, although the conductivities are somewhat lower (10^{-6} S cm^{-1} shortly below the melting point in each case). P_{15}TFSA exhibits only a low temperature, rather low conductivity, ($<10^{-10}$ S cm^{-1}) plateau in its solid state, the conductivity only beginning to rise as the temperature approaches its melting point at P_{16}TFSA appears to have quenched into a glassy state in the conductivity cell. The DSC glass transition temperature of this salt is −87 °C above which point it enters a region where it exists briefly in the deeply supercooled liquid state before crystallizing into the solid state. The same thermal history seems to be present in the conductivity data of figure 2. The low temperature conductivity behaviour around −70 °C is quite different form the other compounds in figure 2 and appears to be a low temperature extension of the room temperature liquid state behaviour. The conductivity of the sample shows a sharp drop around −40 °C, an event that corresponds to a sharp crystallization exotherm in the thermal analysis trace. Thus the drop corresponds to the loss in conductivity in this sample as it forms its solid state, the conductivity dropping to around $10^{-10.5}$ S cm^{-1} before beginning to rise sharply just before the melting point. There appears to be no substantial region of solid state conductivity in this case.

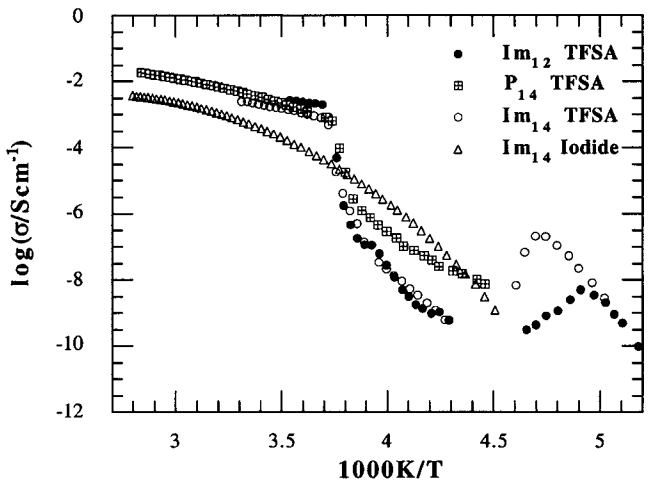

Figure 3. Arrhenius plot of conductivity for a number of low melting point quaternary ammonium TFSA compounds.

Figure 3 compares the conductivity behaviour of a number of related salts of different cations but all of the same anion (TFSA). These salts all contain an ammonium cation, though not necessarily one which is part of a ring as is true of the pyrrolidinium family of figure 2. In this ammonium cation family there are four independently variable alkyl chains and these are denoted by the four subscripts, for example in the nomenclature N_{1114}TFSA. For comparison P_{14}TFSA is also shown. The ammonium cation that would correspond to P_{14}TFSA most closely in terms of number of CH_2 units would be N_{1224}; however since this has not been accessible synthetically thus far, we include a number of ammonium cations of both larger and smaller size in this comparison. Both N_{1114}TFSA and N_{8222}TFSA appear to vitrify in the conductivity experiment. Above their respective glass transitions the conductivity rises rapidly in a liquid-like fashion, the low temperature conduction behaviour being an obvious extension of the molten state behaviour, as described above for P_{16}TFSA. In both cases there

is an obvious drop in conductivity at some higher temperature, as was as was also seen in the case of P_{16}TFSA. Both produce a rapid rise in conductivity again just below their respective melting points. N_{1114}TFSA shows an interesting reproducible drop in conductivity at 9 °C. This coincides with the temperature of the solid–solid transition seen in the thermal analysis trace for this compound. N_{1123}TFSA is relatively featureless in the solid state, the conductivity rising sharply at the melting point from below 10^{-9} S cm^{-1}. By comparison, P_{14}TFSA shows a quite distinct region of solid state conductivity between −50 °C and −17 °C.

One of the distinguishing features of the solid state conduction phenomenon that is obvious in the comparisons in this plot is the concave upwards curvature of conductivity in the solid region of P_{14}TFSA, i.e. the conductivity increase accelerates as the temperature approaches the melting point. Stated in terms of activation energies, P_{14}TFSA *appears* to exhibit an increasing activation energy as temperature increases. In contrast, the typical liquid state behaviour of these salts in their liquid states is the well known [1] concave downwards curvature in this plot, corresponding to a decreasing activation energy with increasing temperature. This distinction is rather revealing; the liquid behaviour is well known to originate from a transport mechanism involving a cooperative rearrangement which requires a critical fluctuation in configurational entropy or free volume [2]. We hypothesize, without further proof at this stage, that an accelerating increase in conductivity with increasing temperature, as seen here in these solid state ion-conductive materials, originates in a rapidly increasing number of active charge carriers. This hypothesis implies a conduction mechanism in which only a small subset of the ions are diffusively active. This mechanism will be discussed in more detail elsewhere [20].

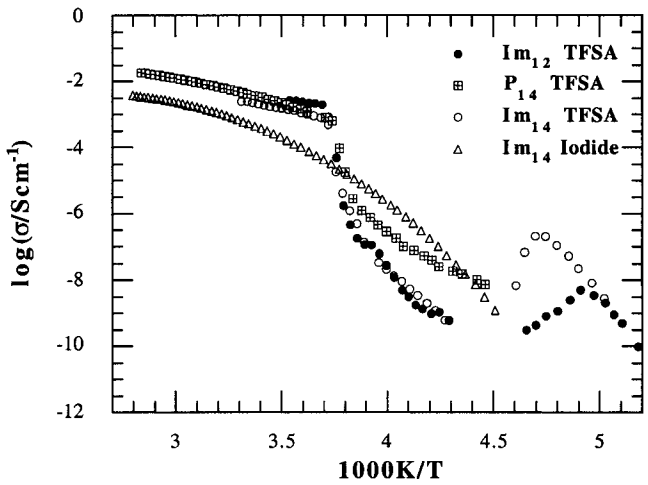

Figure 4. Arrhenius plot of conductivity for several methyl butyl imidazolium and methyl ethyl imidazolium compounds. Note that butyl methyl imidazolium iodide is liquid throughout the temperature range of this experiment.

Figure 4 compares P_{14}TFSA with a number of analogous imidazolium salts (i.e. salts of the methyl butyl imidazolium (Im_{14}) and methyl ethyl imidazolium (Im_{12}) cations). The P_{14} and Im_{14} cations have similar structures, both containing five membered rings with methyl and butyl substituents. However, the imidazolium ring contains two nitrogens, each bearing one of the substituents. The ring and immediately attached CH_2 groups are planar in this case, whereas the pyrrolidinium ring is not completely planar. All three salts have similar melting points. The conductivity behaviour shows elements in common with the ammonium salts, a glass transition at low temperatures being followed by a crystallization into a solid state of low

conductivity. The Im_{14} iodide is liquid over the whole range of this plot.

4. Discussion

Comparing the various salts in figures 2–4, as well as the accompanying thermal data, it appears that high conductivity in the solid state is not a ubiquitous feature of any single family of compounds. It appears as a phenomenon strongly in the smaller P_{1x}TFSA compounds, but is absent for the larger alkyl substituents (P_{15}TFSA and P_{16}TFSA). The ammonium family of salts of the same anion shows no sign of this behaviour amongst the compounds studied. This suggests that the behaviour is not primarily associated with the anion, which is common to all of these compounds. It is conceivable that the TFSA anion could rotate about the long axis of the molecule; however this would involve considerable displacement of the charged oxygen atoms in this molecule and as such could be expected to involve a high activation energy. The molecule would require substantial additional free volume in its vicinity in order to rotate around any of the obvious axes. Thus it appears that the behaviour is more likely to be associated with the cation and, considering the range of cations studied here, the pyrrolidinium ring in particular. This cation is close to planar and has several axes of rotation which might be active in the plastic phases, in particular rotations about an axis normal to the ring. Such a rotation may be possible in the crystalline state with an accessible energy barrier for the smaller alkyl substituents (methyl, ethyl and propyl substituents make only small differences to the overall bulk of the molecule). However for larger values of x, eg the P_{16} case, the alkyl side chain may become too bulky to allow free rotation about such an axis and the rotator phases are thus not accessible. The same hypothesis partially explains the absence of plastic crystal phases and solid state conductivity in the ammonium family of compounds (figure 3). These cations tend to be globular to rodlike in shape and rotation about the molecular long axis is an obvious possibility without a high activation barrier. In fact Ikeda and coworkers [7–11] have observed plastic behaviour and ion conduction in salts of similar cations, but involving more symmetrical anions such as Cl^- and SCN^-. These latter compounds have solid–solid transitions into their rotator phases and melting points at much higher temperatures ($T_m > 400$ K) than the present compounds. The lower melting points in the compounds studied here originate from the diffuse nature of the charge on the TFSA ion, producing weaker ion–ion interactions. Thus it appears that while rotatory motions of these ammonium cations are possible, melting interferes before sufficient thermal energy is available to overcome the activation barrier to rotation in these cases.

The same considerations can explain the lack of rotator phase behaviour in the imidazolium compounds studied. There is an obvious similarity between I_{12} and P_{12}, for example, and the former might be expected to exhibit a possible rotation about an axis normal to the ring. In this case the ring is planar; however the two substituents protrude from the ring in that plane and may offer a greater impediment to rotation than they do in the case of the pyrrolidinium cation. Nonetheless, the key feature again is that the melting point of the I_{12}TFSA compound is considerably lower than the P_{12}TFSA analogue and it therefore appears that the melting transition effectively interferes before the independent rotation can begin. The imidazolium cation also possesses a delocalized charge which may be at least partly responsible for the difference in melting points between Im_{12}TFSA and P_{12}TFSA.

The above discussion has focused on the structural origins of the rotator motions. The nexus between these motions and ion conduction is not automatic. Measured and derived diffusion coefficients [7–11, 20] have shown that diffusive motions of the ions are also present in the plastic phases, as one would expect from the Nernst–Einstein equation and the observed conductivity. However, the way that these transport properties arise from the rotator motions is

not clear. The revolving door type mechanism shown to be present in the Li_2SO_4 case does not obviously have applicability in many of the organic ionic compounds. We hypothesize that the origins of the transport processes stem from the occurrence of a variety of types of lattice defect in the plastic phases. Such defects are also responsible for the plastic mechanical properties [13]. Diffusive and conductive motions of ions via lattice vacancy related mechanisms are well known in the solid state, the key parameter being the concentration of the vacancies [1]. Such vacancies can be expected to be present at a much higher concentration in the plastic phase since energetically it is much closer to the liquid state. The effective thermodynamic cost in vacancy formation, corresponding to the free energy change in transporting a molecular ion from the interior of a crystalline grain to its surface or disordered boundary region, is reduced if (a) interactions are weaker because of molecular rotations, and/or (b) the vacancy formation itself promotes or enables the rotatory motions of neighbouring molecules in the plastic phase. In some cases there is an obvious onset of conduction at the solid–solid transition point. For example P_{11}TFSA is not conductive (i.e. $\sigma < 2.5 \times 10^{-11}$ S cm^{-1}, the measurement limit) below its solid–solid transformation temperature of 20 °C, the conductivity rising sharply to 2×10^{-9} S cm^{-1} as the material enters the higher temperature phase. Thereafter the conductivity rises with temperature at a rate reflecting an apparent activation energy of 60 kJ mol^{-1}, a value quite concordant with vacancy related ion conduction in the solid state. In other cases some of the solid–solid phase transitions do not directly produce a large change in conductivity. For example, P_{12}TFSA appears to enter a conductive phase at -90 °C and then shows only small steps in conductivity, or a change in slope of conductivity against temperature, as it passes through the two higher temperature solid–solid phase transitions. These observations presumably indicate that the structural changes that occur at the phase transition are not directly or substantially altering the concentration of vacancies.

5. Conclusions

The appearance of plastic crystal behaviour among the family of related TFSA salts studied in this work is far from ubiquitous. It appears, from the comparisons made between a number of structurally similar compounds, that plastic crystal behaviour in the TFSA family of salts is primarily associated with the pyrrolidinium ring. This ring is more easily rotated than ammonium compounds of similar size. The appearance of a substantial region of temperature over which a plastic crystal phase is stable also requires that the interionic interactions are sufficiently strong to produce a crystal structure that is energetically stable enough to remain the lowest energy state, despite the presence of the rotatory motions in the plastic phases. The imidazolium TFSA salts exemplify the situation where the electrostatic ionic interactions are sufficiently weak that the material melts before entering a rotator phase.

References

[1] Forsyth M and MacFarlane D R 1999 *Wiley Encyclopedia of Electrical and Electronics Engineering* vol 6 (New York: Wiley) pp 408–18
[2] Gray F M 1991 *Solid Polymer Electrolytes* (New York: VCH) p 13
[3] Angell C A and McLin M G 1992 *Solid State Ion.* **53–56** 1027
[4] Adachi G-Y, Imanaka N and Aono H 1996 *Adv. Mater.* **8** 127–34
[5] MacFarlane D R, Meakin P, Sun J, Amini N and Forsyth M 1999 *J. Phys. Chem.* B **103** 4164–70
[6] Cooper E I and Angell C A 1986 *Solid State Ion.* **18/19** 570–6
[7] Shimizu T, Tanaka S, Onoda-Yamamuro N, Ishimaru S and Ikeda R 1997 *J. Chem. Soc. Faraday Trans.* **93** 321–6
[8] Tanabe T, Nakamura D and Ikeda R 1991 *J. Chem. Soc. Faraday Trans.* **87** 987–90

[9] Handa D, Helmes J H and Majumdar A 1994 *J. Electrochem. Soc.* **141** 1921–7
[10] Hattori M, Fukada S, Nakamura D and Ikeda R 1990 *J. Chem. Soc. Faraday Trans.* **86** 3777–83
[11] Ishida H, Furukawa Y, Kashino S, Sato S and Ikeda R 1996 *Ber. Bunsenges. Phys. Chem.* **100** 433–9
[12] MacFarlane D R, Huang J and Forsyth M 1999 *Nature* **402** 792–4
[13] Timmermans 1961 *J. Phys. Chem. Solids* **18** 1–18
[14] Aronson R *et al* 1980 *J. Physique* C6 **41** 35–7
Aronson R, Knape H E G and Torell L M 1982 *J. Chem. Phys.* **77** 677
Borgesson L and Torell L M 1985 *Phys. Rev.* B **32** 2471–7
[15] Forsyth M, Huang J and MacFarlane D R 2000 *J. Mater. Chem.* **10** 2259–65
[16] Sun J, Forsyth M and MacFarlane D R 1997 *Ionics* **3** 356
[17] Sun J, Forsyth M and MacFarlane D 1998 *J. Phys. Chem.* **102** 8858
[18] Bonhote P, Dias A-P, Papageorgiou N, Kalyanasundaram K and Gratzel M 1996 *Inorg. Chem.* **35** 1168
[19] Golding J, Hamid H, MacFarlane D R, Forsyth M, Forsyth C, Collins C and Huang J 2001 *Chem. Mater.* **13** 558–64
[20] Every H *et al PhD Thesis*